Phase-locking of multiple magnetic droplets by a microwave magnetic field

Chengjie Wang, , Dun Xiao, , Yan Zhou, , J. Åkerman, and , and Yaowen Liu

---

Articles you may be interested in

The design and verification of MuMax3
AIP Advances **4**, 107133 (2014); 10.1063/1.4899186

Current-driven skyrmion motion along disordered magnetic tracks
AIP Advances **7**, 056017 (2017); 10.1063/1.4975658

Low operational current spin Hall nano-oscillators based on NiFe/W bilayers
Applied Physics Letters **109**, 242402 (2016); 10.1063/1.4971828

Current-induced multiple domain wall motion modulated by magnetic pinning in zigzag shaped nanowires
AIP Advances **7**, 056014 (2017); 10.1063/1.4975129

Laser induced ultrafast magnetization reversal in TbCo film
AIP Advances **7**, 056018 (2017); 10.1063/1.4975659

Scaling effect of spin-torque nano-oscillators
AIP Advances **7**, 056624 (2017); 10.1063/1.4974014

Phase-locking of multiple magnetic droplets by a microwave magnetic field

Chengjie Wang,[1] Dun Xiao,[1] Yan Zhou,[2] J. Åkerman,[3,4] and Yaowen Liu[1,a]

[1]*Shanghai Key Laboratory of Special Artificial Microstructure Materials and Technology, School of Physics Science and Engineering, Tongji University, Shanghai 200092, China*
[2]*Department of Physics, The University of Hong Kong, Hong Kong, China*
[3]*Materials Physics, School of Information and Communication Technology, KTH Royal Institute of Technology, Electrum 229, 16440 Kista, Sweden*
[4]*Department of Physics, University of Gothenburg, 412 96 Gothenburg, Sweden*

Manipulating dissipative magnetic droplet is of great interest for both the fundamental and technological reasons due to its potential applications in the high frequency spin-torque nano-oscillators. In this paper, a magnetic droplet pair localized in two identical or non-identical nano-contacts in a magnetic thin film with perpendicular anisotropy can phase-lock into a single resonance state by using an oscillating microwave magnetic field. This resonance state is a little away from the intrinsic precession frequency of the magnetic droplets. We found that the phase-locking frequency range increases with the increase of the microwave field strength. Furthermore, multiple droplets with a random initial phase can also be synchronized by a microwave field. © 2017 Author(s). All article content, except where otherwise noted, is licensed under a Creative Commons Attribution (CC BY) license (http://creativecommons.org/licenses/by/4.0/). [http://dx.doi.org/10.1063/1.4975660]

I. INTRODUCTION

Spin-torque oscillators (STOs)[1] have attracted considerable attentions with the potential of enabling novel spintronic devices for telecommunication and logic applications.[2–7] The STOs are typically fabricated in two different architectures: Nano-pillar[1] or nanoscale electrical contacts (NC)[8] to ferromagnetic thin films with a free magnetic layer and a fixed spin polarizer layer. The spin-transfer torque (STT) in such contacts can compensate the damping torque and excite steady state spin precession in the free layer at a threshold d.c. current. In free layers with perpendicular magnetic anisotropy (PMA), the STT has been predicted to induce a localized oscillation mode—dissipative magnetic droplet soliton.[9,10] Recent experiments have confirmed this type of localized oscillation soliton mode generated in NC region,[11–15] which has been considered as a promising candidate for the STOs. In such devices, the energy dissipation due to magnetic damping is compensated by the energy input from the current-induced STT effect.[16,17] The typical droplet has a partially reversed magnetization directly underneath the NC and all the spins at the NC perimeter rotate in phase around the film normal with a large of precession angle, which can lead to an increase in the microwave output power of NC-STOs by a factor of 40 compared to those of non-droplet counterparts.[11,18] However, this enhanced power is still too weak (~200 pW) for practical applications. Increasing output power of STO is essential for successful adaptation of the STT excitation scheme for advanced microwave oscillators. One promising approach to increasing the output power has been suggested by using the phase-locking mode of an array of STOs through the synchronization technique.[3,19–28] This is a very challenging issue for the droplet-based NC-STOs due to the strongly non-linear soliton property of the magnetic droplets.

---

[a]Corresponding author. Email: yaowen@tongji.edu.cn

To gain insight into the nature of droplet dynamics, micromagnetic simulations have been powerful tools.[9,29–32] In this paper, by employing microwave (MW) magnetic fields, we show that two magnetic droplets formed at identical or non-identical NCs can phase-lock into a single resonance state over a frequency range close to the MW driving frequency. Furthermore, multiple droplets distributed in a 4×4 spatial matrix can also synchronize into a phase-locking state.

II. MODEL

As shown in Fig. 1(a), we consider a NC-STO geometry based on a pseudo spin-valve structure[11,12] patterned into a square shape with 512×512 nm^2. The spin polarizer layer is assumed to be magnetized along the $+z$ direction and the 5-nm thick free layer has perpendicular magnetic anisotropy (PMA). The free layer has two NCs with a separation distance of 240 nm. Positive current is defined as the flow of electrons from the free layer to the polarizer layer.

Micromagnetic modeling of the free layer was performed using the open-source simulation software MuMax3,[33] which is based on the Landau-Lifshitz-Gilbert equation including the STT term:[16,34]

$$\frac{d\mathbf{m}}{dt} = -\gamma \mathbf{m} \times \mathbf{H}_{eff} + \alpha \mathbf{m} \times \frac{d\mathbf{m}}{dt} + a_J \mathbf{m} \times (\mathbf{m} \times \mathbf{m}_f)$$

The magnetization $\mathbf{m} = \mathbf{M}/M_S$, M_S is the saturation magnetization. The first term describes the spin precession, the second term is the Gilbert damping term, the third one is the Slonczewski STT term[16] that only works on the NC region. a_J is the STT strength. The effective magnetic field $\mathbf{H}_{eff}$ includes the exchange field, anisotropy field, demagnetization field (magnetic dipole interaction), and external magnetic field. In this study, the external magnetic field contains a static magnetic field $\mathbf{H}_0$ applied in z-direction and a microwave (MW) magnetic field $\mathbf{H}_{MW} = H_{MW,0} \sin(2\pi f_{MW} t) \hat{\mathbf{e}}_y$ applied in y-direction, where $H_{MW,0}$ is the field strength and f_{MW} is the MW frequency. The following material parameters measured on similar Co/Ni multilayers are used for the free layer:[11,14] $M_s = 716$ kA/m (saturation magnetization), $K_u = 447$ kJ/m^3 (magnetic anisotropy), $A = 30$ pJ/m (exchange stiffness), $\alpha = 0.05$ (Gilbert damping), $P = 0.5$ (spin polarization). The applied current is 8 mA for each NC except the case of specific notation in this study. The current-induced Oersted field is not taken into account for most simulations. $\mu_0 H_0 = 0.8$ T along z axis, which results in the Zeeman precession frequency $f_0 = \gamma H \approx 22.5$ GHz consequently. In order to reduce the influence of sample boundary, a periodic boundary condition is used in both x-direction and y-direction. In this study, all the simulations are performed at zero temperature.
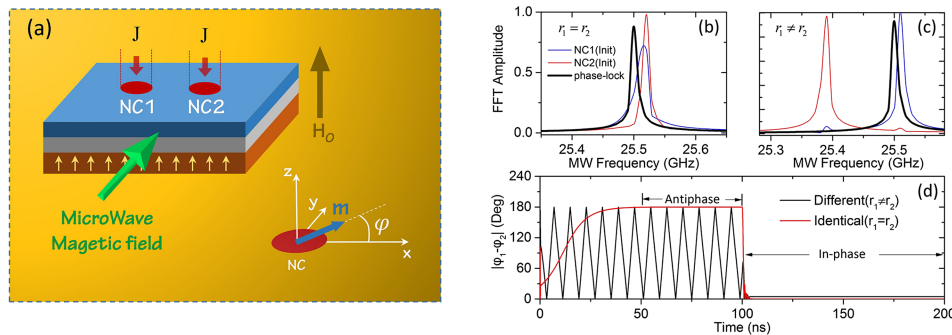

FIG. 1. (a) Schematic diagram of NC-STOs. φ is the angle between the in-plane magnetization and x-axis. FFT spectra calculated from $<m_x>$ of droplets for two identical NCs (b) and for two non-identical NCs (c). The initial frequencies for NC1 and NC2 are indicated by the thin blue and red curves, respectively. The phase-locking frequency driven by the MW field is given by the black curve. (d) Time dependent phase difference between the two droplets for identical and non-identical cases, respectively.

III. SIMULATION RESULTS

A. Synchronization of two droplets at identical NCs

Figs. 1(b)–(d) show the typical dynamics of droplet pairs driven by a microwave magnetic field, in which the ac MW magnetic field is applied along y-axis direction with the amplitude of 20 mT and the frequency of 25.50 GHz. First, a droplet pair is generated at two identical NCs ($r_1 = r_2$ = 15 nm) by applying a current of 8 mA flowing in each NC. The details of creation process of a droplet pair can be found in our previous study.[32] Simulation indicates that the magnetization precession of the two droplets have almost same intrinsic frequency of ~25.52 GHz, as the thin curves shown in Fig. 1(b). Here the frequencies are calculated from time dependent m_x using the fast Fourier transform (FFT) technique. In our simulations, we set the two droplets having different initial magnetization phase ($\varphi_1 \neq \varphi_2$), where φ is the angle of the in-plane magnetization component of droplet at the NC circumference with the *x*-axis. The phase difference $\Delta\varphi = |\varphi_1 - \varphi_2|$ of the droplet pair first will slightly increase to an antiphase magnetization precession state ($\Delta\varphi \approx 180°$), see Fig. 1(d). When an AC microwave magnetic field $\mathbf{H}_{MW}$ is switched on at $t = 100$ ns, the droplet pair with the antiphase state is quickly locked into an in-phase synchronization precession state ($\Delta\varphi \approx 0°$) within 2 ns (see movie S1 of the supplementary material), at which the two droplets start to rotate with a frequency of 25.50 GHz same as that of the driving microwave field as shown in Fig. 1(b).

We would like to point out that the appearance of antiphase precession state in double or multiple NCs driven by STT effect is a normal feature, which has been suggested three possible reasons:[23,24] The dynamic dipole-dipole interaction (DDI), spin wave (SW), or the separation distance between the two droplets. In order to clarify which factor plays the role for the antiphase state, we have carried out a series of simulations by switching on/off the DDI, SW, and current-induced Oersted-field. Also the separation distance varies from 240 nm to 260 nm. We find that without the microwave magnetic field the antiphase precession state is a favorite state with the DDI and SW effect (not shown). This antiphase state only disappears at relative large separation distance and with the Oersted field case. This result is consistent well with the experiments.[27]

The phase-locking state of the droplet pair depends on the microwave driving field. Fig. 2(a) shows the FFT output frequency of the droplet pair as a function of the microwave source, where the driving source is fixed to be 20 mT and the frequency varies from 24 GHz to 27 GHz (correspondingly to ±1.5 GHz away from the intrinsic frequency of a droplet). Fig. 2(b) shows the time dependent phase difference of the two droplets. Note that the two droplets can quickly phase-lock into a synchronization state when the source frequency changing from 24.8 GHz to 26.2 GHz. In this region, the two droplets are locked into the frequency of driving source, resulting in a resonance state between the droplet pair and the source. The frequency difference between the droplet and microwave source is smaller than a specific value (~0.7 GHz). This behavior is similar to that theoretically predicted by Slavin and Tiberkevich,[23] in which the phase of magnetization is tuned by the combined effect from an oscillating stray field and a spin wave. In addition, the NC2 droplet has a larger synchronization range in frequency with the driving MW source, as shown in Fig. 2(a). Our simulations show that the large microwave field may enlarge the droplet diameter somehow, resulting in one of the droplet is larger than the other even for them generated at same size of NCs (see movie S2 of the supplementary material). It is noticed that the intrinsic frequency of droplet decreases with the increase of droplet diameter,[9,32] therefore, the window of frequency locking for NC2 is larger than that of NC1. However, it is unclear why the droplets generated at NC1 and NC2 have the different response to the MW driving source. For the relative small microwave driving source, this phenomenon will disappear. We would like to point out that the phase-locking (PL) window in Fig. 2(a) is defined as the frequency region both the two droplets having the same frequency as well as the same precession phase (or a fixed phase difference).

The phase-locking window is also manipulated by the strength of driving magnetic fields. Fig. 2(c) shows the phase-locking feature by tuning the microwave source strength from 2 mT to 20 mT. Obviously, the stronger of driving source, the wider of phase-locking range. For the field strength smaller than 2 mT, the phase-locking range is smaller than 200 MHz. Another important feature
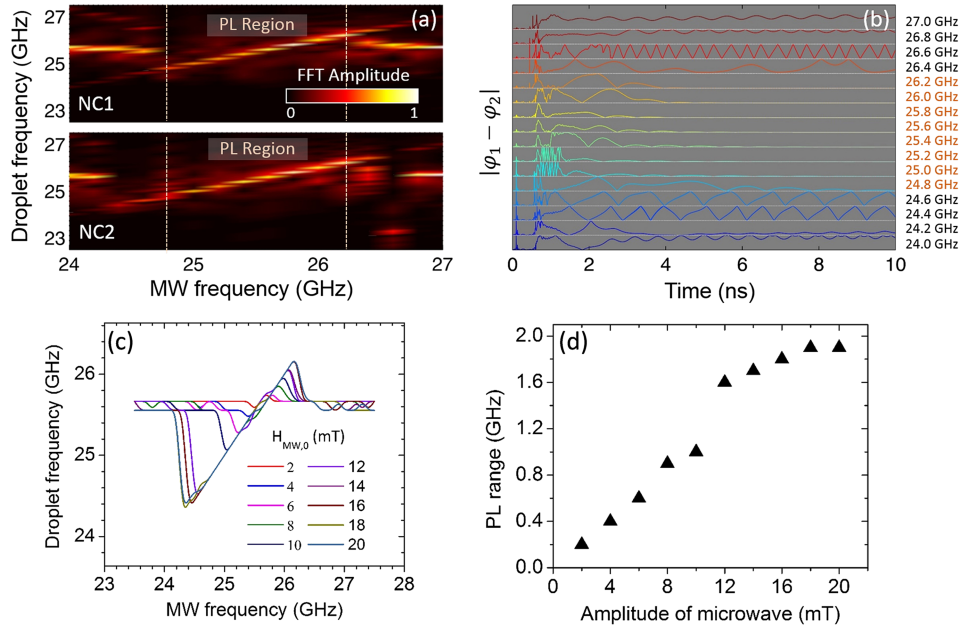
FIG. 2. Phase-locking (PL) of a droplet pair at two identical NCs driven by a microwave magnetic field. (a) Frequency analysis by FFT as a function of the driving source frequency. (b) The phase difference v.s. time. The curves are offset vertically for clarity. The microwave driving source changes from 24 GHz to 27 GHz. (c) The dependence of phase-locking region on the microwave strength. (d) The phase-locking difference $\Delta f = f_{max} - f_{min}$ depends on the microwave strength.

shown in Fig. 2(c) is that the phase-locking range is asymmetry, showing the different response of the droplet pair to high-frequency and low-frequency driving signals. The droplet pair prefers to resonate with the low-frequency microwave fields. Fig. 2(d) summarizes the phase-locking difference Δf as a function of the strength of microwave fields, where Δf is defined as the difference between the upper and lower bounds of phase-locking frequency, $\Delta f = f_{max} - f_{min}$. Note that, the Δf linearly increases with the microwave strength for $H < 10$mT. Interestingly, there is a pronounced jump between 10 and 18 mT, which may correspond to a new type of precession mode excitation. But the underlying physics for this jump is unclear. After that, the Δf is saturated to be 1.8 GHz. This saturated frequency interval is originated from the topological protection of droplet structure.

B. Synchronization of a droplet pair at non-identical NCs

In contrast, for a droplet pair formed at different size of NCs ($r_1 = 16.5$ nm, $r_2 = 15$ nm), the synchronization process demonstrates significant different behaviors. Firstly, the two droplets have different intrinsic frequencies in absence of the MW magnetic fields, showing the big droplet ($r_1 = 16.5$ nm) has a little lower intrinsic frequency of 25.38 GHz [Fig.1(c)]. This can be attributed to the increased droplet size, the frequency decreases with the increase of radius size.[9,32] Secondly, the transient phase difference $\Delta\varphi$ before the synchronization state featured a drastic oscillation between 180° and 0°, as shown in Fig. 1(d). However, when the MW driving field is switched on at $t = 100$ ns, the magnetization precession of the two droplets synchronizes with each other very quickly, with a same frequency (25.5 GHz) and a fixed phase difference $\Delta\varphi \approx 4.6°$. Thirdly, due to the non-identical size, the phase-locking frequency window of the two droplets is shrunk a little [see Fig. 3(a)]. Moreover, a nonzero stable $\Delta\varphi$ value is observed for this phase-locking state, and the $\Delta\varphi$ increases with the frequency of microwave increasing, as shown in Fig. 3(b). In addition, we would like to point out that for the droplet pair at two non-identical NCs having too large different intrinsic frequencies (e.g. induced by big difference of NC size), the phase-locking will be invalid.
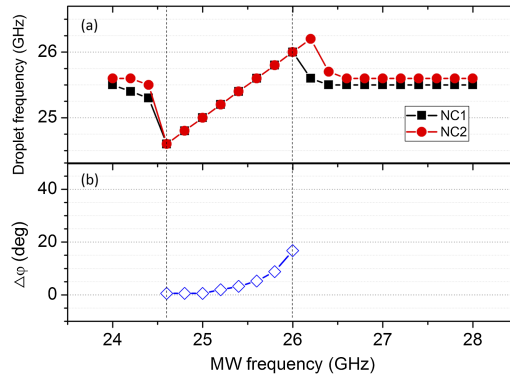
FIG. 3. The phase-locking of a droplet pair at two non-identical NCs ($r_1 = 16.5$ nm, $r_2 = 15$ nm) driven by a microwave magnetic field of 20 mT. (a) Phase-locking frequency; (b) Phase difference $\Delta\varphi$.
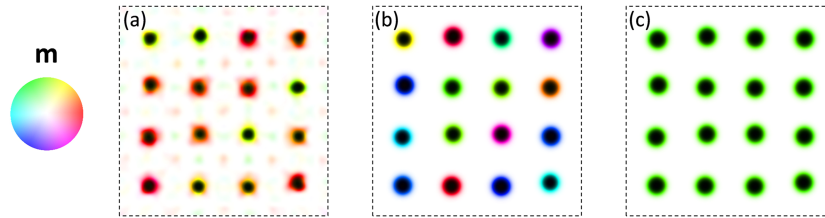

FIG. 4. Phase-locking of multiple droplets by microwave driving field, $H_{MW,0} = 20$ mT, $f_{MW} = 25.5$ GHz. Phase configuration of the droplet matrix at (a) t=0 ns, the initial state; (b) t = 10 ns, without MW field; (c) t = 10 ns, with the MW field. The color disk on the left represents the direction of the magnetization.

C. Synchronization of multiple droplets

Synchronization of multiple droplets is also available by using the microwave magnetic field. Fig. 4 shows the simulation results for a matrix of 4×4 droplets performed with or without the microwave driving source. The separation distance between the neighbor NCs is 240 nm. In this simulation, a random initial droplet state is firstly generated at each NC by applied d.c. current. These droplets have different initial phase angle φ, see Fig. 4(a). Without the microwave magnetic field, these droplets have never to be locked in phase state as the time increases, as shown in Fig. 4(b). However, when the microwave field is switched on, we can see that all the droplets with the different initial phase can be quickly synchronized into an in-phase state with a same phase-locking frequency of 25.5 GHz, see Fig. 4(c) and movie S3 of the supplementary material.

IV. CONCLUSION

In summary, we show that droplet-based NC-STOs can be synchronized by using a microwave field. The phase-locking range can be tuned by the microwave field strength, showing the range increases with the field strength. An asymmetry phase-locking window is observed, because the droplet pair prefers to synchronize with the relatively lower frequency of the microwave source, compared with the intrinsic precession frequency of the droplet. Multiple droplets formed in a 4×4 NC matric can also be synchronized by the microwave magnetic field.

SUPPLEMENTARY MATERIAL

See the supplementary material for showing the process of the phase-locking two identical droplets (movies S1 and S2) and multiple droplets (movie S3).

[1] S. I. Kiselev, J. C. Sankey, I. N. Krivorotov, N. C. Emley, R. J. Schoelkopf, R. A. Buhrman, and D. C. Ralph, Nature **425**, 380 (2003).

[2] I. N. Krivorotov, N. C. Emley, J. C. Sankey, S. I. Kiselev, D. C. Ralph, and R. A. Buhrman, Science **307**, 228 (2005).

[3] J. Grollier, V. Cros, and A. Fert, Phys. Rev. B **73**, 060409 (2006).

[4] T. J. Silva and W. H. Rippard, J. Magn. Magn. Mater. **320**, 1260 (2008).

[5] A. Brataas, A. D. Kent, and H. Ohno, Nat.Mater. **11**, 372 (2012).

[6] Z. Zeng, G. Finocchio, and H. Jiang, Nanoscale **5**, 2219 (2013).

[7] G. Bertotti, C. Serpico, I. D. Mayergoyz, A. Magni, M. d'Aquino, and R. Bonin, Phys. Rev. Lett. **94**, 127206 (2005).

[8] W. H. Rippard, M. R. Pufall, S. Kaka, T. J. Silva, and S. E. Russek, Phys. Rev. B **70**, 100406 (2004).

[9] M. A. Hoefer, T. J. Silva, and M. W. Keller, Phys. Rev. B **82**, 054432 (2010).

[10] M. A. Hoefer, M. Sommacal, and T. J. Silva, Phys. Rev. B **85**, 214433 (2012).

[11] S. M. Mohseni, S. R. Sani, J. Persson, T. N. A. Nguyen, S. Chung, Y. Pogoryelov, P. K. Muduli, E. Iacocca, A. Eklund, R. K. Dumas, S. Bonetti, A. Deac, M. A. Hoefer, and J. Åkerman, Science **339**, 1295 (2013).

[12] F. Macià, D. Backes, and A. D. Kent, Nature Nanotech. **9**, 992 (2014).

[13] M. D. Maiden, L. D. Bookman, and M. A. Hoefer, Phys. Rev. B **89**, 180409 (2014).

[14] E. Iacocca, R. K. Dumas, L. Bookman, M. Mohseni, S. Chung, M. A. Hoefer, and J. Åkerman, Phys. Rev. Lett. **112**, 047201 (2014).

[15] S. M. Mohseni, S. R. Sani, R. K. Dumas, J. Persson, T. N. Anh Nguyen, S. Chung, Y. Pogoryelov, P. K. Muduli, E. Iacocca, A. Eklund, and J. Åkerman, Physica B: Condensed Matter **435**, 84 (2014).

[16] J. C. Slonczewski, J. Magn. Magn. Mater. **159**, L1 (1996).

[17] L. Berger, Phys. Rev. B **54**, 9353 (1996).

[18] S. Chung, S. M. Mohseni, S. R. Sani, E. Iacocca, R. K. Dumas, T. N. Anh Nguyen, Y. Pogoryelov, P. K. Muduli, A. Eklund, M. Hoefer, and J. Åkerman, J. Appl. Phys. **115**, 172612 (2014).

[19] S. Kaka, M. R. Pufall, W. H. Rippard, T. J. Silva, S. E. Russek, and J. A. Katine, Nature **437**, 389 (2005).

[20] F. B. Mancoff, N. D. Rizzo, B. N. Engel, and S. Tehrani, Nature **437**, 393 (2005).

[21] R. Sharma, P. Dürrenfeld, E. Iacocca, O. G. Heinonen, J. Åkerman, and P. K. Muduli, Appl. Phys. Lett. **105**, 132404 (2014).

[22] M. Carpentieri, T. Moriyama, B. Azzerboni, and G. Finocchio, Appl. Phys. Lett. **102**, 102413 (2013).

[23] Y. Zhou, J. Persson, S. Bonetti, and J. Akerman, Appl. Phys. Lett. **92**, 092505 (2008).

[24] X. Chen and R. H. Victora, Phys. Rev. B **79**, 180402 (2009).

[25] P. Tabor, V. Tiberkevich, A. Slavin, and S. Urazhdin, Phys. Rev. B **82**, 020407 (2010).

[26] S. Urazhdin, P. Tabor, V. Tiberkevich, and A. Slavin, Phys. Rev. Lett. **105**, 104101 (2010).

[27] A. Houshang, E. Iacocca, P. Durrenfeld, S. R. Sani, J. Akerman, and R. K. Dumas, Nat Nanotechnol **11**, 280 (2016).

[28] A. D. Belanovsky, N. Locatelli, P. N. Skirdkov, F. A. Araujo, J. Grollier, K. A. Zvezdin, V. Cros, and A. K. Zvezdin, Phys. Rev. B **85**, 100409 (2012).

[29] G. Finocchio, V. Puliafito, S. Komineas, L. Torres, O. Ozatay, T. Hauet, and B. Azzerboni, J. Appl. Phys. **114**, 163908 (2013).

[30] V. Puliafito, L. Torres, O. Ozatay, T. Hauet, B. Azzerboni, and G. Finocchio, J. Appl. Phys. **115**, 17D139 (2014).

[31] C. Moutafis, S. Komineas, and J. A. C. Bland, Phys. Rev. B **79**, 224429 (2009).

[32] D. Xiao, Y. Liu, Y. Zhou, S. M. Mohseni, S. Chung, and J. Åkerman, Phys. Rev. B **93**, 094431 (2016).

[33] A. Vansteenkiste, J. Leliaert, M. Dvornik, M. Helsen, F. Garcia-Sanchez, and B. Van Waeyenberge, AIP Advances **4**, 107133 (2014).

[34] X. Li, Z. Zhang, Q. Y. Jin, and Y. Liu, New J. Phys. **11**, 023027 (2009).